ORIGINAL ARTICLE

Redefining the Manual Wheelchair Stroke Cycle: Identification and Impact of Nonpropulsive Pushrim Contact

Andrew M. Kwarciak, MS, Sue Ann Sisto, PT, PhD, Mathew Yarossi, BS, Robert Price, MSME, Eugene Komaroff, PhD, Michael L. Boninger, MD

ABSTRACT. Kwarciak AM, Sisto SA, Yarossi M, Price R, Komaroff E, Boninger ML. Redefining the manual wheelchair stroke cycle: identification and impact of nonpropulsive pushrim contact. Arch Phys Med Rehabil 2009;90:20-6.

Objectives: To create a comprehensive definition of the manual wheelchair stroke cycle, which includes multiple periods of pushrim contact, and to show its improved clinical benefit to wheelchair propulsion analyses.

Design: Cross-sectional biomechanics study.

Setting: Three motion analysis laboratories.

Participants: Persons (N=54) with paraplegia who use a manual wheelchair.

Interventions: Not applicable.

Main Outcome Measures: Pushrim forces, axle moments, and contact angles measured during wheelchair propulsion.

Results: Total force on the pushrim was used to define pushrim contact and positive axle moment was used to identify the included period of propulsive contact. During most strokes, periods of nonpropulsive contact existed before and after propulsive contact. Within these periods, braking moments were applied to the pushrim, resulting in negative power output, or power loss. Including nonpropulsive data decreased mean stroke moment and power. The magnitude and the angle over which braking moments and power loss occurred increased with wheel speed. Mean braking moment and power loss within the initial contact period were significantly ($P<.001$) related to stroke pattern.

Conclusions: The proposed definition of the stroke cycle provides a thorough and practical description of wheelchair propulsion. Researchers and clinicians should use this definition to understand and minimize the impact of nonpropulsive contact throughout the stroke.

From Kessler Medical Rehabilitation Research and Education Center, West Orange, NJ (Kwarciak, Sisto, Yarossi, Komaroff); Department of Physical Medicine and Rehabilitation, University of Medicine and Dentistry of New Jersey, New Jersey Medical School, Newark, NJ (Sisto, Komaroff); Department of Rehabilitation Science, Stony Brook University, Stony Brook, NY (Sisto); Department of Rehabilitation Medicine, University of Washington, Seattle, WA (Price); Human Engineering Research Laboratories, Veterans Affairs Pittsburgh Healthcare System, Pittsburgh, PA (Boninger); Departments of Bioengineering and Rehabilitation Science and Technology, University of Pittsburgh, Pittsburgh, PA (Boninger); Department of Physical Medicine and Rehabilitation, University of Pittsburgh Medical Center Health System, Pittsburgh, PA (Boninger).

Presented to the Rehabilitation Engineering and Assistive Technology Society of North America, June 15–19, 2007, Phoenix, AZ.

Supported by the National Institute on Disability and Rehabilitation Research (grant no. H133A011107) and by the Henry H. Kessler Foundation.

No commercial party having a direct financial interest in the results of the research supporting this article has or will confer a benefit on the authors or on any organization with which the authors are associated.

Reprint requests to Andrew M. Kwarciak, MS, Kessler Medical Rehabilitation Research and Education Center, 1199 Pleasant Valley Way, West Orange, NJ 07052, e-mail: *akwarciak@kesslerfoundation.net.*

0003-9993/09/9001-00213$36.00/0
doi:10.1016/j.apmr.2008.07.013

Key Words: Biomechanics; Rehabilitation; Wheelchair.

THE HIGH PREVALENCE of upper-limb pain and pathology in manual wheelchair users[1-6] has given rise to a growing area of research in wheelchair propulsion mechanics. Numerous studies have reported the kinetics and kinematics of propulsion[7-9]; and have suggested ways to improve propulsion efficiency and reduce the risk of overuse injury.[10-13] As this research continues to develop, the tools used to evaluate wheelchair propulsion must be improved to permit more detailed and precise analyses. One of the most fundamental and underdeveloped aspects of wheelchair propulsion analyses is the definition of the propulsive stroke, or the stroke cycle.

The stroke cycle has been described as having 2 phases: push and recovery. The push phase is defined as the period when the hand is in contact with the pushrim and applying force to the pushrim to maintain or increase wheelchair velocity, while the recovery phase is the period between consecutive push phases when the arms are retracted in preparation for another push.[14] These phases are analogous to the stance and swing phases described in the gait cycle. Both sets of phases describe a repeating sequence of unilateral loading and unloading of distal segments to facilitate mobility. However, unlike the simple, 2-phase stroke cycle, the gait cycle includes a detailed subdivision of stance and swing into 3 functional tasks: weight acceptance, single limb support, and limb advancement, and a further subdivision into 8 phases of gait.[15] This detailed phasic description of gait has provided clinicians and researchers the means to study differences in gait across multiple patient types and to determine how a disability or injury may affect specific aspects of gait. It is this level of precision and detail that is missing from the current definition of the manual wheelchair stroke cycle.

A key deficiency of the current stroke cycle definition has been the inconsistent and exclusive description of the push phase. Previous studies of wheelchair propulsion have used pushrim forces,[10,12,16-20] moments,[9,21-23] or both forces and moments[24,25] to describe the push phase. Force indicates when the hand is in contact with the pushrim, whereas a moment, particularly a moment about the axle, indicates when force is applied tangentially to the pushrim. The study of axle moments is typically limited to moments that result in forward movement of the wheelchair; however, several studies have reported negative moments before and after propulsion.[21,26,27] Negative axle moments, generated during forward propulsion, result

List of Abbreviations

KMRREC	Kessler Medical Rehabilitation Research and Education Center
SCI	spinal cord injury

from nonoptimal coupling between the hand and the spinning pushrim and can be exacerbated by muscular and sensory impairments.[27] Though they are not considered part of the push phase, negative moments may influence the effectiveness of forward propulsion.

To better describe wheelchair propulsion, standardize analyses, and improve clinical value, a precise, more widely accepted definition of the stroke cycle is needed. The objective of this study was to create a comprehensive definition of the stroke cycle, focusing on the interval of pushrim contact, and to show the clinical usefulness of the new definition. To redefine the stroke cycle, measurements of total force on the pushrim and axle moment were used to properly establish the limits of pushrim contact and to identify periods of propulsive and nonpropulsive contact. Measurements of axle moment and calculations of mean contact angles and power output were provided to show the importance of considering phases of nonpropulsive contact.

To show the importance and clinical utility of the new definition, an analysis involving stroke patterns was performed to determine if axle moment and power output within the newly established periods of pushrim contact could detect differences in stroke pattern. Although the path of the hand is typically confined to the pushrim during the push phase, the movement of the hand before and after pushrim contact has been correlated to mechanical efficiency.[10,11,28] This suggests that stroke patterns may influence propulsion biomechanics at the beginning and end of the push phase. A new definition of the stroke cycle, with precise subdivisions, would provide clinicians and researchers with a greater opportunity to understand and study the effects of stroke pattern, and other variables or conditions, on wheelchair propulsion.

METHODS

We obtained data from a multi-center study on upper-limb pain and pathology in manual wheelchair use. The centers included Kessler Medical Rehabilitation Research and Education Center, West Orange, New Jersey, the Human Engineering Research Laboratories, University of Pittsburgh, Pittsburgh, Pennsylvania, and the Department of Rehabilitation Medicine, University of Washington, Seattle, Washington.

Participants

Fifty-nine persons with paraplegia were recruited for this study. To qualify for participation, subjects were required to have an SCI below T1, be between 18 and 65 years of age, use a manual wheelchair as their primary means of mobility, be at least 1 year postinjury, have sustained their SCI after the age of 18 (or after reaching skeletal maturity), and use 24-in rear wheels with quick-release axles to ensure compatibility with the instrumented wheels used for testing. Candidates were excluded if they had a history of upper limb trauma, sustained an upper-limb injury from which they had not fully recovered, suffered from pain as a result of a syrinx or complex regional pain syndrome, or if they were pregnant. All participants provided written and informed consent for the study as approved by the respective center's institutional review board prior to initiation of data collection.

Data Collection

Participants were asked to propel their own wheelchairs on a 2-drum roller system at a self-selected speed and a target speed of 1.8m/s. Wheel speed was measured with a tachometer on each roller and displayed with a custom Labview[a] program on a computer monitor placed in front of the participant. The rear wheels of the chairs were replaced with a pair of SmartWheels.[b] The Department of Rehabilitation Medicine, University of Washington, used a single SmartWheel attached to the nondominant side. The SmartWheel is an instrumented wheel that measures angular position and velocity of the wheel, and the 3-dimensional forces and moments applied to the pushrim during propulsion. For all trials, SmartWheel data were recorded at 240Hz. Raw voltages were filtered with an eighth-order, zero phase, low-pass Butterworth filter with a 20-Hz cutoff frequency[29] and converted into forces and moments about the anterior-posterior, medial-lateral, and superior-inferior axes. Attachment of the SmartWheels did not affect rear wheel camber, which was measured on the original wheels with a digital inclinometer.

Spherical reflective markers (KMRREC and Department of Rehabilitation Medicine, University of Washington) or active LED markers (Human Engineering Research Laboratories, University of Pittsburgh) were fixed to bony landmarks on the head, trunk, and upper limb, and on the axle of each SmartWheel. Marker trajectories were recorded with a Vicon[c] motion capture system at KMRREC, an Optotrak[d] motion capture system at the Human Engineering Research Laboratories, University of Pittsburgh, and a Qualisys[e] motion capture system at the Department of Rehabilitation Medicine, University of Washington at 60Hz or 120Hz. All trials collected at 120Hz were down-sampled by selecting every other data point. Marker trajectories were filtered using a second-order, zero phase, low-pass Butterworth filter with a 6-Hz cutoff frequency.[30] Each trial lasted 20 seconds and began once the participant reached a consistent, self-selected speed. For the 1.8m/s target speed condition, each trial began once the participant maintained a speed within 0.22m/s (12%) of the target speed.

Data Reduction and Analysis

We used data recorded from the left side of each participant to create and test the proposed definition. Data from 5 participants were removed from the analysis, 3 due to SD in the total force baseline that exceeded 1N, and 2 due to hysteresis in total force. Kinematic data were limited to the markers on the axle of the SmartWheel and the third metacarpal-phalangeal joint (hand). Using measurements of rear wheel camber, all forces, moments, and marker trajectories were rotated into the global reference frame. This was done to normalize for camber and to improve stroke pattern classification. All trials contained at least 6 strokes. In some trials, a section of data containing erroneous spikes was removed from the beginning or end of the trial.

Kinetics

Previously filtered data obtained from the SmartWheel were filtered a second time with an eighth-order, zero phase, 20-Hz low-pass Butterworth filter to enhance baseline noise removal. The component forces (F_x, F_y, and F_z) were summed to compute total force on the pushrim (F_{tot}):

$$F_{tot} = \sqrt{(F_x^2 + F_y^2 + F_z^2)}$$

Total force on the pushrim was used to represent force instead of any single component force because it considers force in any direction. Axle moments were represented by the opposite of the moment about the SmartWheel z-axis.

The limits of the total force on the pushrim and axle moment were determined by applying a threshold to each signal. Each threshold was created from sections of the signal when the hand was off the pushrim (force and moment measurements oscillated about zero). Twenty points of data from each section

were combined and averaged to determine the baseline noise. For total force on the pushrim, 3 SDs were added to the baseline noise to create the threshold of detection (2.97±1.56N). The limits of the total force on the pushrim were the first and last points at which the total force on the pushrim exceeded the threshold. For strokes in which the total force on the pushrim spiked above the threshold directly before or after the main contact force, the limits were expanded to include the additional force spikes. For axle moment, 3 SDs were added to and subtracted from the baseline noise to create an upper (0.38±0.14Nm) and lower (−0.38±0.14Nm) threshold of detection. Axle moment began once it crossed either threshold and ended on the point before it returned to a value between the thresholds. Axle moment was referred to as a propulsive moment when it exceeded the upper threshold and as a braking moment when it dropped below the lower threshold. All limit detections were performed objectively with a custom Matlab[f] program. Visual inspection was used to verify the selections made by the program, but no changes were made to any of the selected data points.

To show the importance of precisely and consistently identifying pushrim contact, we performed calculations of mean contact time, mean contact angle, and power over the limits of total force on the pushrim and axle moment. These calculations are typical in wheelchair propulsion analyses and may be affected by the limits of pushrim contact. Using data from the SmartWheel, the time and angle over which total force on the pushrim and axle moment occurred were computed. The external power output on the wheel was computed by the equation:

$$Power = \frac{M_{ax} \times V_w}{R_w}$$

where M_{ax} equals axle moment, V_w equals the linear velocity of the wheel and R_w equals the wheel radius. Data from 2 speed conditions were used to confirm the findings and to determine the effect of speed on the calculations.

Stroke Pattern

An analysis of stroke pattern was included to determine if the proposed definition provided a better evaluation of propulsion kinematics. Stroke patterns describe the movement of the hand during the recovery phase of the stroke. Four distinct patterns have been identified: pumping or arcing, semi-circular, single-looping over propulsion, and double-looping over propulsion[10,28] (fig 1). Several studies have supported the semi-circular pattern, which

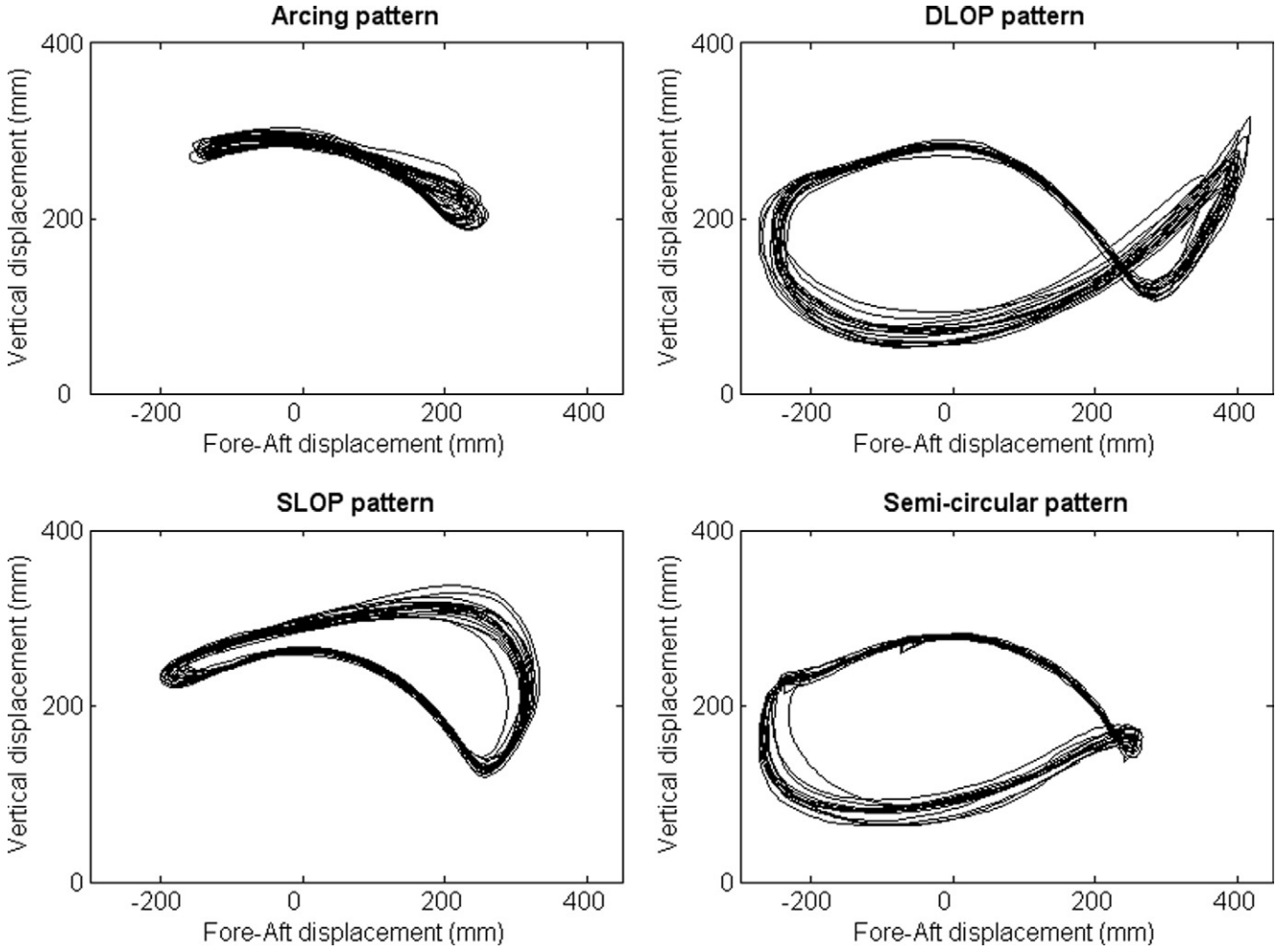

Fig 1. Four classic stroke patterns (clockwise from upper left): arcing, DLOP, semi-circular, and SLOP. The arcing and SLOP patterns were classified as over-rim propulsive strokes while the semi-circular and DLOP patterns were classified as under-rim propulsive strokes. Abbreviations: DLOP, double-looping over propulsion; SLOP, single-looping over propulsion.

has been associated with lower stroke frequency[28] and less angular joint velocity and acceleration on release of the pushrim.[10] These findings are part of a clinical guideline for the preservation of upper limb function after SCI.[31] The guideline regards stroke pattern as one of several modifiable parameters that can impact upper-limb health.

For this study, 3 independent reviewers, with different levels of experience in wheelchair propulsion analysis, visually inspected sagittal plane hand marker trajectories and described each using 1 of the 4 patterns. To simplify the stroke pattern distinctions, the single-looping over propulsion and arcing patterns were referred to as over-rim propulsive strokes and the double-looping over propulsion and semi-circular patterns were referred to as under-rim propulsive strokes. This classification removes the subjectivity associated with stroke pattern identification and places more emphasis on how the hand is expected to approach the pushrim during initial contact. These 2 consolidated patterns were used to explore differences in axle moment and power within the limits of total force on the pushrim and axle moment. Only data from the self-selected speed condition were used to determine the effect of stroke pattern. All calculations and stroke pattern analyses were performed in Matlab.

Statistics

Paired Student *t* tests were used to: (1) compare the limits of total force on the pushrim with the limits of axle moment, (2) compare phase angles across the 2 speed conditions, and (3) compare mean axle moment and power across the periods of pushrim contact. Independent *t* tests were also used to evaluate differences in mean axle moment and power within each period across the 2 stroke pattern classifications. Alpha was adjusted for 40 multiple comparisons and set at 0.001. Statistical analyses were performed using SAS software.[g]

RESULTS

Participants

Fifty-four persons (44 men, 10 women) with chronic paraplegia (average duration of injury, 14.4±10.4y) participated in the analysis. The mean age was 40.7±11.3 years and the mean weight was 76.6±16.4kg. Injury levels ranged from T2 to L1.

Temporal and Spatial Limits of the Contact Phase

Threshold-based detection algorithms were applied to measurements of total force on the pushrim and axle moment to produce 2 estimates of pushrim contact, or the "contact phase." The term contact phase is preferred to the traditionally used "push phase" in order to distinguish the new definition and to help differentiate propulsive contact from nonpropulsive contact. Under both speed conditions, the differences in the 2 sets of onset and cessation times were significant ($P<.001$). At the self-selected speed (1.08±0.31m/s), total force on the pushrim was detected 0.016±0.021 seconds before the onset of axle moment and 0.015±0.019 seconds beyond the cessation of axle moment. At the 1.8m/s target speed (1.74±0.21m/s), total force on the pushrim was detected 0.016±0.017 seconds before the onset of axle moment and 0.017±0.019 seconds beyond the cessation of axle moment. Differences in this timing occurred in about one third of all strokes. In terms of the angle over which total force on the pushrim and axle moment were applied, the total force angle was 6.35±5.81° larger than the axle moment angle at 1.08m/s and 9.04±9.24° larger at 1.74m/s.

Subdividing the Contact Phase

Based on the inclusive limits of total force on the pushrim and the development of propulsive moment, the limits of total force on the pushrim were used to define the contact phase and the limits of propulsive moment were used to subdivide the contact phase into periods of propulsive (propulsion) and nonpropulsive (initial contact and release) contact (fig 2). The initial contact period, representing hand contact without propulsive moment, was defined as the interval between the onset of total force on the pushrim and the onset of propulsive moment. The propulsion period was defined as the interval between the onset and cessation of propulsive moment. The release period, representing hand contact without propulsive moment, was defined as the interval between the cessations of propulsive moment and total force on the pushrim. The recovery phase was the interval when no force was present.

Nonpropulsive Contact within the Initial Contact and Release Periods

Within the initial contact and release periods, non-propulsive contact between the hand and the spinning pushrim often led to the generation of a braking moment. A braking moment was detected in the initial contact period of 70% of all strokes at 1.08m/s and 88% of all strokes at 1.74m/s. Likewise, a braking moment was detected in the release period, at both speeds, in 43% and 63% of all strokes, respectively. The angles over which braking moment were generated composed a majority of the initial contact and release period angles. Table 1 shows the angle of each contact period and braking moment at each speed. As wheel speed increased from 1.08m/s to 1.74m/s, the initial contact period braking moment angle increased 87% and the release period braking moment angle increased 101%.

Impact of Nonpropulsive Contact on Axle Moment and Power

Axle moment and power, within each period of the contact phase, are presented in table 2. All comparisons of axle moment and power both within and across speeds were significant

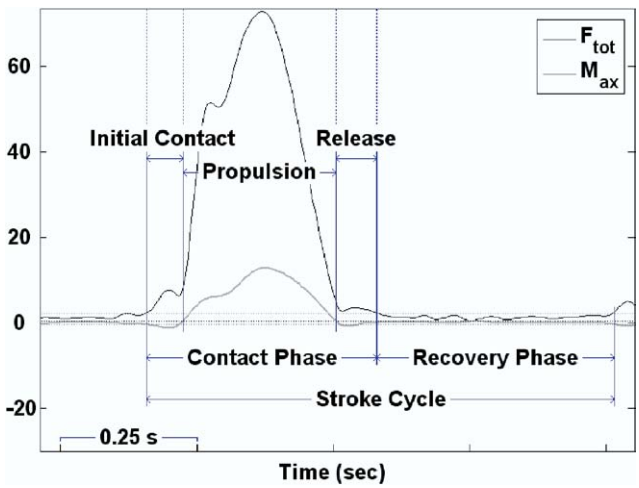

Fig 2. Proposed subdivision of pushrim contact. The contact phase begins when F_{tot} exceeds its threshold and ends when F_{tot} drops back below its threshold. The generation of a propulsive moment divides the contact phase into the initial contact, propulsion, and release periods. The recovery phase constitutes the remainder of the stroke cycle, when no F_{tot} is detected. Abbreviations: F_{tot}, total force on the pushrim; M_{ax}, axle moment.

Table 1: Mean Angle of Each Period Within the Contact Phase for Each Speed

Period	Angle (degrees)	
	1.08m/s	1.74m/s
Initial contact	9.55±5.68	16.08±6.56
(Initial contact M_b)	(6.91±4.63)	(12.92±5.94)*
Propulsion	80.64±15.68	81.04±13.93
Release	8.19±4.65	14.86±7.43
(Release M_b)	(4.47±4.29)	(8.98±6.07)*

NOTE. Values are mean ± SD. Initial Contact M_b and Release M_b indicate the angle over which a braking moment occurred in each period.
Abbreviation: M_b, braking moment about the axle.
*Significantly ($P<.001$) higher than value at 1.08m/s.

($P<.001$). At each speed, braking moments and negative power (power loss) were measured in both the initial contact and release periods. Inclusion of data from these 2 periods caused a drop in mean stroke axle moment and power. In other words, by considering nonpropulsive contact in the initial contact and release periods, when axle moment and power are negative, calculations of axle moment and power for the entire stroke were significantly lower than those of the propulsion period alone. At the self-selected speed, contact phase axle moment and power were 13.6% lower than propulsion period axle moment and power. As wheel speed increased, the differences in axle moment and power between the overall contact phase and the included propulsion period rose to 23%. Statistical comparisons across both speeds are provided in table 2.

Stroke Pattern

The propulsion patterns used by the participants affected the way tangential force was applied to the pushrim. Table 3 shows the mean axle moment and power for the self-selected speed, broken down by stroke pattern. Due to inconsistencies in stroke patterns within the trial, data from 2 participants were excluded. Participants who used an under-rim stroke (n=26) had a significantly ($P<.001$) smaller braking moment and power loss during the initial contact period than participants who used an over-rim stroke (n=26). Power loss during initial contact was about 2.6 times greater in the over-rim stroke group.

Table 2: Mean Axle Moment and Power in the Contact Phase and Each Period Within the Contact Phase at Each Speed

Phase/Period	Axle Moment (Nm)	
	1.08m/s	1.74m/s
Contact	7.79±2.53*	8.36±2.91*
Initial contact	−0.36±0.29	−0.62±0.40
Propulsion	8.98±2.75	10.79±3.32
Release	−0.17±0.21	−0.37±0.30
	Power (W)	
Contact	28.25±14.44*	47.87±16.81*
Initial contact	−1.10±0.92	−3.29±2.12
Propulsion	32.84±16.96	61.84±19.90
Release	−0.71±0.87	−2.21±1.83

NOTE. Values are mean ± SD. Axle moment and power were calculated as the mean values in each period; therefore, the mean values of the 3 periods do not sum to the contact phase mean. All 1.74m/s values were significantly different ($P<.001$) than their comparable 1.08m/s values.
*Significantly lower ($P<.001$) than propulsion period.

Table 3: Mean Axle Moment and Power in Each Period of the Contact Phase for Each Stroke Pattern at the Self-Selected Speed Condition

Period	Axle Moment (Nm)		Power (W)	
	Over-Rim	Under-Rim	Over-Rim	Under-Rim
Initial contact	−0.53±0.29	−0.19±0.18*	−1.64±0.92	−0.62±0.61*
Propulsion	9.32±2.57	8.72±3.01	33.72±12.88	32.96±20.62
Release	−0.15±0.18	−0.19±0.24	−0.63±0.70	−0.81±1.03

NOTE. Values are mean ± SD. The over-rim stroke group had a mean speed of 1.08m/s, while the under-rim stroke group had a mean speed of 1.11m/s.
*Significantly ($P<.001$) less negative than over-rim stroke value in the initial contact period.

DISCUSSION

A new definition of the manual wheelchair stroke cycle was created to better describe wheelchair propulsion, to help establish consistency across studies, and to improve clinical merit. The definition was based on quantitative measurements of wheelchair propulsion. Unlike the original and still current definition of the stroke cycle, which was established through visual inspection of wheelchair use, the proposed definition used technology that has proven valuable to both the research and the clinical community. The use of an instrumented wheel, such as the SmartWheel, enabled us to establish the precise limits and subdivisions of pushrim contact, thus improving the accuracy and applicability of the stroke cycle definition.

The first step in creating the proposed definition was to determine the appropriate limits of the contact phase. Paired *t* tests revealed that the limits of axle moment fell significantly within the limits of total force on the pushrim at each speed. Therefore, the contact phase was defined by the limits of total force on the pushrim. Although it is unclear from their descriptions, some studies appear to have used deviations in component forces, with and without component moments, to determine the limits of the pushrim contact.[7,18,24,25] It is possible that component forces may have been detected beyond the limits of total force; however, variability in the force measurements would have prevented accurate threshold-based detection. When component forces and moments are used, their limits are often determined by visual inspection. This method is sufficient for analyses of peak variables within the stroke, but not for precise onset and cessation detection. Visual inspection is subjective and has not been evaluated for its repeatability. The threshold-based detection algorithm provided an objective and repeatable method of determining the contact phase.

With the limits of contact established, the detection of propulsive moments was used to distinguish propulsive contact from nonpropulsive contact. This distinction is important to understand the effectiveness of pushrim contact and to reveal how variables, such as wheel speed and stroke pattern, affect propulsive and nonpropulsive contact. While the majority of the contact phase was dedicated to propulsion, significant periods (initial contact and release) were composed of nonpropulsive contact. By incorporating data from the initial contact and release periods, the new definition provides a basis from which to study the causes and effects of nonpropulsive contact.

In applying the new definition of the stroke cycle, nonpropulsive contact had a significant impact on phase angles, axle moments, and power output. At each speed condition, the initial contact and release periods represented significant portions of the contact angle. Within each of these periods, significant braking moments and power loss were generated. As wheel speed increased, the size and magnitude of the braking moments and power loss increased. This was attributed to the

decreased efficiency in grasping and releasing a faster spinning pushrim. A slower, yet functional, speed may help wheelchair users reduce the magnitude of braking moments and power loss. When the braking moments and power loss from the initial contact and release periods were averaged in with the propulsion period values, mean axle moment and power decreased significantly. Therefore, inclusion of data from the initial contact and release periods in calculations of stroke moment and power are critical to ensure accurate and consistent results.

In addition to providing a better description of propulsion kinetics, braking moments and power loss within the initial contact period were related to differences in propulsion kinematics. Participants that used an under-rim stroke had significantly less initial contact braking moment and power loss than participants who used an over-rim stroke. This is consistent with the results of a study by de Groot et al[11] on the effect of stroke pattern on mechanical efficiency and propulsion technique. The study found that the semi-circular pattern (under-rim stroke) resulted in smaller negative deflections in axle moment prior to propulsion than either the arcing or single-looping over propulsion pattern (over-rim strokes). These results did not translate into gross mechanical efficiency, which was highest using the arcing pattern. Despite the conclusion that power loss before and after propulsion might have been too small to significantly affect gross mechanical efficiency, the finding should not be disregarded. Braking moments and power loss in the initial contact period may affect the rate and efficiency of force application during the subsequent propulsion period. By including negative axle moments, along with positive axle moments and total force, the proposed definition of the stroke cycle provides a better way to evaluate the effect of different stroke styles.

Understanding braking moments and power loss, within the context of kinematic behavior, could lead to improved wheelchair propulsion training. While dropping the hand below the pushrim during recovery does not guarantee more effective force application, the data show this approach to be more advantageous than keeping the hand above the rim. This supports the recommendation of the clinical guideline that wheelchair users allow their hands to drift down naturally, keeping them below the pushrim during recovery.[31] Wheelchair users can achieve this hand movement using the semi-circular pattern or the double-looping over propulsion pattern. Clinicians should consider these findings when training people in wheelchair propulsion. Any improvements to the propulsive stroke, no matter how small, can help preserve upper-limb health in wheelchair users. Although the braking moments and power loss detected during the initial contact and release periods had relatively small magnitudes and durations, they hindered forward propulsion and, for any given person, could constitute a much larger proportion of the contact phase; to ignore these events would be imprudent. Further research is required to determine the impact of nonpropulsive contact on propulsion efficiency and joint loading.

The proposed definition of the stroke cycle should be adopted to standardize and improve propulsion analyses. As Perry stated in one of the first papers on the mechanics of walking, "For the clinician to use the scientist's findings, the data must be reinterpreted into functional terminology and concepts."[32] The new definition of the stroke cycle, modeled from the gait cycle,[15,33] describes the stroke with a functional breakdown of phases and contact periods (fig 3). Its comprehensive description provides the means to study nonpropulsive contact and to help clinicians and researchers develop ways to optimize wheelchair propulsion and reduce the risk of pain and injury to the upper limbs. Future investigations may consider proposing a subdivision of the recovery phase into distinct periods (eg, follow-through, return, and approach) that would permit better evaluation of joint loading throughout the remainder of the stroke cycle.

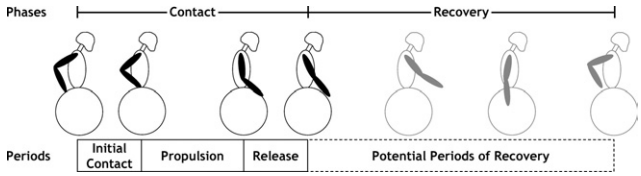

Fig 3. The new definition of the stroke cycle. The stroke is divided into the contact phase and the recovery phase; and the contact phase is subdivided into the initial contact, propulsion, and release periods. An indication of potential recovery periods is made as future research may lead to a subdivision of the recovery phase. Adapted from Perry[15] and Sutherland et al.[33]

Study Limitations

There are several limitations to this study. First, data were collected in an artificial environment. The use of a roller system and SmartWheels, which require participants to push only on the pushrims, may have affected propulsion biomechanics and data collection. Also, the nature of the propulsion, straight forward at a steady velocity, is not indicative of typical wheeling that involves stopping, turning, and maneuvering over and around obstacles. Despite its limited assessment of wheelchair use, the protocol established consistency across subjects and allowed us to record kinematics and pushrim kinetics during consecutive push strokes. In addition, the use of the SmartWheels is justified by its proven value to research[34-37] and growing popularity in seating and mobility clinics as a tool for evaluating wheelchairs, wheelchair setups, and wheelchair propulsion over a variety of surfaces. Second, selection bias may have affected the results. This study used a convenience sample of subjects; thus the results may lack generalizablity or external validity. Also, some data were removed from the analysis due to high noise content or inconsistencies. The selection of data was objective and focused on including as much useable data as possible. Third, not all of the data appeared normally distributed. To assess the impact of skew or flatness on our P values, statistical analyses were also run with Wilcoxon nonparametric tests. There were no substantive changes in conclusions; all null hypotheses that were rejected with the t tests were also significantly rejected with the nonparametric analog of the t tests. Lastly, in terms of the comparisons between axle moment and power across the different stroke pattern groups, uncontrolled variables, such as sensory capabilities, strength, and wheelchair configuration could have affected the results. The analysis of axle moment and power across stroke pattern was performed on previously collected data. A future, targeted study may help isolate the effect of stroke pattern and other factors such as wheelchair setup on propulsive and nonpropulsive pushrim contact.

CONCLUSIONS

The existing definition and method for determining the manual wheelchair stroke cycle ignores important details and is inadequate; it underserves researchers and clinicians seeking to understand wheelchair propulsion. The proposed definition of the stroke cycle provides a more precise and comprehensive description of wheelchair propulsion. By identifying the intervals of propulsive and nonpropulsive contact, the definition clearly describes the propulsion period and the transitions between propulsion and recovery. Within these transition periods, wheelchair users are prone to inefficient coupling of the

hand to the pushrim, leading to the development of braking moments and power loss. The magnitude and size of the braking moments and power loss were related to wheel speed and, in the initial contact period, to stroke pattern. Researchers and clinicians must consider the periods of nonpropulsive contact and how they impact overall stroke power and efficiency. The proposed definition of the stroke cycle establishes the terminology and means to evaluate the effects of both propulsive and non-propulsive contact throughout the stroke.

References

1. Nichols PJ, Norman PA, Ennis JR. Wheelchair user's shoulder? Shoulder pain in patients with spinal cord lesions. Scand J Rehabil Med 1979;11:29-32.
2. Sie IH, Waters RL, Adkins RH, Gellman H. Upper extremity pain in the postrehabilitation spinal cord injured patient. Arch Phys Med Rehabil 1992;73:44-8.
3. Subbarao JV, Klopfstein J, Turpin R. Prevalence and impact of wrist and shoulder pain in patients with spinal cord injury. J Spinal Cord Med 1995;18:9-13.
4. Dalyan M, Cardenas DD, Gerard B. Upper extremity pain after spinal cord injury. Spinal Cord 1999;37:191-5.
5. Curtis KA, Drysdale GA, Lanza RD, Kolber M, Vitolo RS, West R. Shoulder pain in wheelchair users with tetraplegia and paraplegia. Arch Phys Med Rehabil 1999;80:453-7.
6. Jensen MP, Hoffman AJ, Cardenas DD. Chronic pain in individuals with spinal cord injury: a survey and longitudinal study. Spinal Cord 2005;43:704-12.
7. Rodgers MM, Tummarakota S, Lieh J. Three-dimensional dynamic analysis of wheelchair propulsion. J Appl Biomech 1998;14:80-92.
8. Boninger ML, Cooper RA, Robertson RN, Shimada SD. Three-dimensional pushrim forces during two speeds of wheelchair propulsion. Am J Phys Med Rehabil 1997;76:420-6.
9. Kulig K, Rao SS, Mulroy SJ, et al. Shoulder joint kinetics during the contact phase of wheelchair propulsion. Clin Orthop Relat Res 1998(354):132-43.
10. Shimada SD, Robertson RN, Bonninger ML, Cooper RA. Kinematic characterization of wheelchair propulsion. J Rehabil Res Dev 1998;35:210-8.
11. de Groot S, Veeger HE, Hollander AP, van der Woude LH. Effect of wheelchair stroke pattern on mechanical efficiency. Am J Phys Med Rehabil 2004;83:640-9.
12. Kotajarvi BR, Sabick MB, An KN, Zhao KD, Kaufman KR, Basford JR. The effect of seat position on wheelchair propulsion biomechanics. J Rehabil Res Dev 2004;41:403-14.
13. Richter WM, Rodriguez R, Woods KR, Axelson PW. Stroke pattern and handrim biomechanics for level and uphill wheelchair propulsion at self-selected speeds. Arch Phys Med Rehabil 2007;88:81-7.
14. Sanderson DJ, Sommer HJ, 3rd. Kinematic features of wheelchair propulsion. J Biomech 1985;18:423-9.
15. Perry J. Gait analysis: normal and pathological function. Thorofare: Slack Inc; 1992.
16. Finley MA, Rasch EK, Keyser RE, Rodgers MM. The biomechanics of wheelchair propulsion in individuals with and without upper-limb impairment. J Rehabil Res Dev 2004;41:385-95.
17. Sabick MB, Kotajarvi BR, An KN. A new method to quantify demand on the upper extremity during manual wheelchair propulsion. Arch Phys Med Rehabil 2004;85:1151-9.
18. Veeger HE, Rozendaal LA, van der Helm FC. Load on the shoulder in low intensity wheelchair propulsion. Clin Biomech (Bristol, Avon) 2002;17:211-8.
19. Newsam CJ, Rao SS, Mulroy SJ, Gronley JK, Bontrager EL, Perry J. Three dimensional upper extremity motion during manual wheelchair propulsion in men with different levels of spinal cord injury. Gait Posture 1999;10:223-32.
20. van Drongelen S, van der Woude LH, Janssen TW, Angenot EL, Chadwick EK, Veeger DH. Mechanical load on the upper extremity during wheelchair activities. Arch Phys Med Rehabil 2005;86:1214-20.
21. Dallmeijer AJ, van der Woude LH, Veeger HE, Hollander AP. Effectiveness of force application in manual wheelchair propulsion in persons with spinal cord injuries. Am J Phys Med Rehabil 1998;77:213-21.
22. Koontz AM, Cooper RA, Boninger ML, Souza AL, Fay BT. Shoulder kinematics and kinetics during two speeds of wheelchair propulsion. J Rehabil Res Dev 2002;39:635-50.
23. Boninger ML, Cooper RA, Robertson RN, Rudy TE. Wrist biomechanics during two speeds of wheelchair propulsion: an analysis using a local coordinate system. Arch Phys Med Rehabil 1997;78:364-72.
24. Mercer JL, Boninger M, Koontz A, Ren D, Dyson-Hudson T, Cooper R. Shoulder joint kinetics and pathology in manual wheelchair users. Clin Biomech (Bristol, Avon) 2006;21:781-9.
25. Yang YS, Koontz AM, Triolo RJ, Mercer JL, Boninger ML. Surface electromyography activity of trunk muscles during wheelchair propulsion. Clin Biomech (Bristol, Avon) 2006;21:1032-41.
26. de Groot S, Veeger DH, Hollander AP, van der Woude LH. Wheelchair propulsion technique and mechanical efficiency after 3 wk of practice. Med Sci Sports Exerc 2002;34:756-66.
27. Fay BT, Boninger ML, Fitzgerald SG, Souza AL, Cooper RA, Koontz AM. Manual wheelchair pushrim dynamics in people with multiple sclerosis. Arch Phys Med Rehabil 2004;85:935-42.
28. Boninger ML, Souza AL, Cooper RA, Fitzgerald SG, Koontz AM, Fay BT. Propulsion patterns and pushrim biomechanics in manual wheelchair propulsion. Arch Phys Med Rehabil 2002;83:718-23.
29. Cooper RA, DiGiovine CP, Boninger ML, Shimada SD, Robertson RN. Frequency analysis of 3-dimensional pushrim forces and moments for manual wheelchair propulsion. Automedica 1998;16:355-65.
30. Cooper RA, DiGiovine CP, Boninger ML, Shimada SD, Koontz AM, Baldwin MA. Filter frequency selection for manual wheelchair biomechanics. J Rehabil Res Dev 2002;39:323-36.
31. Preservation of upper limb function following spinal cord injury: a clinical practice guideline for health-care professionals. J Spinal Cord Med 2005;28:434-70.
32. Perry J. The mechanics of walking. A clinical interpretation. Phys Ther 1967;47:778-801.
33. Sutherland DH, Olshen RA, Biden EN, Wyatt MP. The development of mature walking. London: MacKeith Pr; 1988.
34. Cowan RE, Boninger ML, Sawatzky BJ, Mazoyer BD, Cooper RA. Preliminary outcomes of the SmartWheel Users' Group database: a proposed framework for clinicians to objectively evaluate manual wheelchair propulsion. Arch Phys Med Rehabil 2008;89:260-8.
35. Price R, Ashwell ZR, Chang MW, Boninger ML, Koontz AM, Sisto SA. Upper-limb joint power and its distribution in spinal cord injured wheelchair users: steady-state self-selected speed versus maximal acceleration trials. Arch Phys Med Rehabil 2007;88:456-63.
36. Koontz AM, Yang Y, Price R, et al. Multisite comparison of wheelchair propulsion kinetics in persons with paraplegia. J Rehabil Res Dev 2007;44:449-58.
37. Richter WM. The effect of seat position on manual wheelchair propulsion biomechanics: a quasi-static model-based approach. Med Eng Phys 2001 Dec;23:707-12.

Suppliers

a. National Instruments Corp, 11500 N Mopac Expwy, Austin, TX 78759-3504.
b. Three Rivers Holdings LLC, 1826 W Broadway Rd, Ste 43, Mesa, AZ 85206.
c. Vicon, 9 Spectrum Pointe Dr, Lake Forest, CA 92630.
d. Northern Digital Inc, 103 Randall Dr, Waterloo, ON, Canada N2V 1C5.
e. Qualisys AB, Packhusgatan 6, S-411 13 Gothenburg, Sweden.
f. The MathWorks Inc, 3 Apple Hill Dr, Natick, MA 01760-2098.
g. SAS Institute Inc, 100 SAS Campus Dr, Cary, NC 27513-2414.